Noncovalent π Interactions

DOI: 10.1002/ange.201409672

Surfing π Clouds for Noncovalent Interactions: Arenes versus Alkenes**

Abil E. Aliev, Josephine R. T. Arendorf, Ilias Pavlakos, Rafael B. Moreno, Michael J. Porter, Henry S. Rzepa, and William B. Motherwell**

Abstract: *A comparative study of molecular balances by NMR spectroscopy indicates that noncovalent functional-group interactions with an arene dominate over those with an alkene, and that a π-facial intramolecular hydrogen bond from a hydroxy group to an arene is favored by approximately 1.2 kJ mol^{-1}. The strongest interaction observed in this study was with the cyano group. Analysis of the series of groups CH_2CH_3, $CH{=}CH_2$, $C{\equiv}CH$, and $C{\equiv}N$ shows a correlation between conformational free-energy differences and the calculated charge on the C^{α} atom of these substituents, which is indicative of the electrostatic nature of their π interactions. Changes in the free-energy differences of conformers show a linear dependence on the solvent hydrogen bond acceptor parameter β.*

The vital role played by noncovalent interactions, especially the contribution of aromatic rings to chemical and biological recognition, continues to be a subject of intense research activity.[1] Detailed understanding and quantifiable estimates of the strength, distance, and geometric dependence of such intermolecular forces are essential, not only for the understanding of protein–ligand interactions and hence for drug design, but also for the synthesis of new asymmetric ligands, catalysts, and sensors. Phenomena such as π stacking,[2] the behavior of an aromatic ring as a hydrogen-bond acceptor,[3] or cation–π interactions[4] have been studied extensively. Although a variety of techniques have contributed to provide valuable insight, the use of designed molecular balances has proven particularly useful for estimating the very small interaction energies involved. Moreover, such balances also allow the often dominant influence of solvation to be explored. The molecular torsion balance pioneered by Wilcox and co-workers[2d,5] has provided the basic framework for many elegant studies, which exemplify the quantitative power of this approach, and the results from a significant number of new molecular balances[6] have been summarized in an insightful review by Mati and Cockroft.[7]

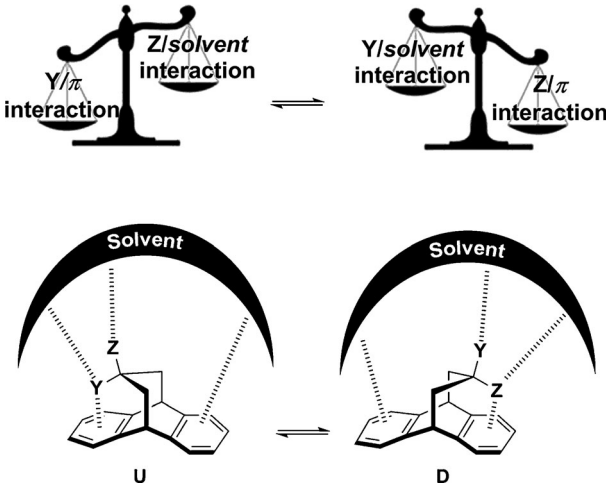

Figure 1. Conformational equilibrium of molecular balances. "U" and "D" denote up and down orientations of the more electronegative substituent Z.

Within this area, we have previously introduced the dibenzobicyclo[3.2.2]nonane framework as a useful probe for the comparative study of arene–functional-group interactions in solution. The two substituents Y and Z (Figure 1) were varied systematically, and the conformational population was measured in each case by NMR spectroscopy.[8] In this manner, interesting insights, such as the "preference" of an aromatic ring for a fluorine atom over a hydroxy group, or the higher affinity of an arene for sulfur over oxygen were gained. It is important to recognize that this bicyclic scaffold is not a torsional balance but a top-pan balance (or seesaw), since, for any given derivative, the influence of Y on the first aromatic ring is being measured against the counterbalancing interaction of Z with the second aromatic ring.

In sharp contrast to the extensive body of work on aromatic systems, however, relatively few studies have quantified noncovalent interactions involving the simplest fundamental π system of all, an alkene.[9] Thus, even though the existence of π-facial hydrogen bonding of a hydroxy group to an alkene has been recognized through infrared dilution studies[10] and X-ray crystallographic database mining,[10b,d,11] a quantifiable comparison of such arene versus alkene noncovalent functional-group interactions has, to the best of our knowledge, not yet been made. Herein, we now present our preliminary measurements of the relative strength of a π-

[*] Dr. A. E. Aliev, Dr. J. R. T. Arendorf, Dr. I. Pavlakos, Dr. R. B. Moreno, Dr. M. J. Porter, Prof. W. B. Motherwell
Department of Chemistry, University College London
20 Gordon Street, London WC1H 0AJ (UK)
E-mail: a.e.aliev@ucl.ac.uk
w.b.motherwell@ucl.ac.uk
Prof. H. S. Rzepa
Department of Chemistry, Imperial College London
South Kensington campus, London, SW7 2AZ (UK)

[**] Support for this work from the Leverhulme Trust is gratefully acknowledged.

Supporting information for this article is available on the WWW under http://dx.doi.org/10.1002/anie.201409672.

 © 2015 Wiley-VCH Verlag GmbH & Co. KGaA, Weinheim

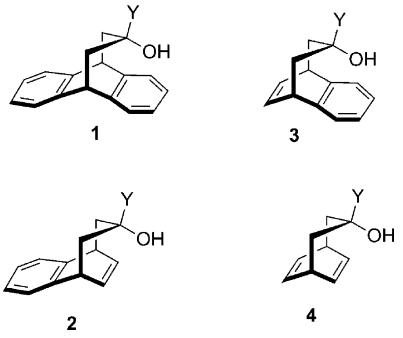

Scheme 1. Molecular balances **1**–**4** (Y = H, Me, Et, CH=CH$_2$, C≡CH, C≡N).

facial intramolecular hydrogen bond to an arene versus an alkene.

As emphasized in Scheme 1, consideration of the requirements for such a comparison leads to the design of four different molecular balances so that measurements can be made relative to an identical counterbalancing interaction. In the present study, for example, a comparison of the OH–arene versus OH–alkene interaction can only be made either relative to a Y–arene interaction (**1** versus **2**) or relative to a Y–alkene interaction (**3** versus **4**), but not by comparing dibenzo derivatives **1** with dienes **4**. As in our earlier study, the population p_D of the OH-down conformer was calculated by using the average coupling constants observed by NMR spectroscopy (see the Supporting Information). The results for the 20 alcohol and 3 cyanohydrin derivatives prepared are compiled in Table 1.

A comparison of the results even by simple visual inspection of the conformational population reveals several features of interest. Thus, as expected, the hydroxy group in all secondary alcohols **1**–**4** with Y = H points towards the solvent, thus indicating that any π-facial hydrogen bond which can be formed in the second conformation cannot compensate for the difference in the van der Waals radii of oxygen and hydrogen. By way of contrast, for all of the tertiary alcohols studied (Y = Me, Et, CH=CH$_2$, C≡CH), pairwise comparison of **1** and **2** clearly indicates that the OH···π-arene interaction is observed to a greater extent than the OH···π-alkene interaction. The same trend is also mirrored, but to a much lesser extent, in the pairwise comparison of the set of derivatives **3** versus **4**, which may be an indication that the counterbalancing Y···π-alkene interaction is much less favorable than the Y···π-arene interaction and decreases in the series Et > Me > CH=CH$_2$ > C≡CH. The fact that this observation is more pronounced in the more polar solvents (to which the hydroxy group can form a hydrogen bond) may be a consequence of the fact that hydrophobic shielding of the OH group by the aromatic ring is more efficient than by the double bond.

Whilst steric effects can certainly dominate the interaction between an alkyl group and a π cloud, it is interesting to note that there is also a trend towards an increasing Y···π interaction as a function of the hybridization of the α-carbon atom with sp^3 < sp^2 < sp, as clearly exemplified by the data for the acetylenic alcohols. Remarkably, for the cyanohydrin derivatives, the interactions of both the alkene and the arene with the cyano group completely dominate over any π-facial intramolecular hydrogen bonding from the hydroxy group, even in nonpolar solvents, possibly as a result of the increasing electrophilic character of the sp-hybridized carbon atom, which is ideally located to benefit from the electron density associated with the π-donors (see below). Once again, for all alkyne derivatives and for the cyano group, interaction with the arene is more favorable than with the alkene.

Table 1: Populations p_D [%] of the OH-down conformer (T = 298 K) in molecular balances **1**, **2**, **3**, and **4** shown in Scheme 1.[a]

	1	**2**	**3**	**4**
			OH | H	
$CDCl_3$	6.4	4.6	12.7	8.7
C_6D_6	3.8	3.2	7.1	5.4
CD_3CN	0.7	0.8	2.3	0.7
CD_3OD	0.0	0.0	0.0	0.0
[D_5]pyridine	1.0	0.9	1.8	0.5
[D_6]DMSO	0.3	0.3	0.6	0.2
			OH | Me	
$CDCl_3$	93.5	92.4	98.8	98.9
C_6D_6	91.0	88.3	97.9	97.8
CD_3CN	76.5	67.9	94.5	93.6
CD_3OD	52.2	41.8	86.3	82.4
[D_5]pyridine	46.3	46.3	83.2	82.2
[D_6]DMSO	43.4	30.1	77.2	71.2
			OH | Et	
$CDCl_3$	98.5	95.8	99.5	99.6
C_6D_6	96.7	95.1	99.3	99.1
CD_3CN	88.9	84.6	97.7	97.2
CD_3OD	75.9	66.4	94.3	92.9
[D_5]pyridine	77.5	72.5	94.1	93.1
[D_6]DMSO	64.4	53.8	89.8	88.2
			OH | CH=CH$_2$	
$CDCl_3$	93.5	88.6	97.7	97.0
C_6D_6	91.3	86.9	96.8	96.3
CD_3CN	80.0	68.4	92.9	91.0
CD_3OD	64.6	53.3	87.0	84.9
[D_5]pyridine	66.4	49.6	84.3	78.1
[D_6]DMSO	57.4	39.9	80.2	72.9
			OH | C≡CH	
$CDCl_3$	50.2	44.3	71.1	68.8
C_6D_6	39.3	31.1	61.0	58.1
CD_3CN	29.8	17.0	53.7	41.1
CD_3OD	17.1	9.8	35.5	23.7
[D_5]pyridine	18.8	8.1	29.1	16.8
[D_6]DMSO	20.8	11.0	31.4	19.6
			OH | C≡N	
$CDCl_3$	24.8	17.8	29.1	–
C_6D_6	20.8	17.5	18.7	–
CD_3CN	2.7	1.2	7.5	–
CD_3OD	0.0	0.0	0.7	–
[D_5]pyridine	2.0	0.5	–	–
[D_6]DMSO	1.2	0.3	0.0	–

[a] The values reported are based on the accuracy of NMR J coupling measurements (±0.05 Hz; see the Supporting Information); the error in the p_D values is estimated to be within ±0.9%. DMSO = dimethyl sulfoxide.

© 2015 Wiley-VCH Verlag GmbH & Co. KGaA, Weinheim

In general terms, the solvent dependence of molecular balances **1**–**4** follows the expected trend, with less polar solvents favoring a much higher population p_D of the conformers featuring a π-facial intramolecular hydrogen bond.

For the more polar solvents CD_3CN, CD_3OD, [D_5]pyridine, and [D_6]DMSO, which can form strong but instantaneous hydrogen bonds with the hydroxy group, the observed changes in the p_D and $\Delta G°$ values (see Table S4 in the Supporting Information) correlate very well with the hydrogen bond acceptor parameter β, as shown in Figure 2 for the series **1**–**4**, Y = Me (see also Table S7 for further data). They do not correlate, however, with the dielectric constant ε (see Table S6), and further detailed scrutiny of the solvation data on the basis of the α/β electrostatic solvent competition model developed by Hunter will certainly be of interest.[6b,12,13]

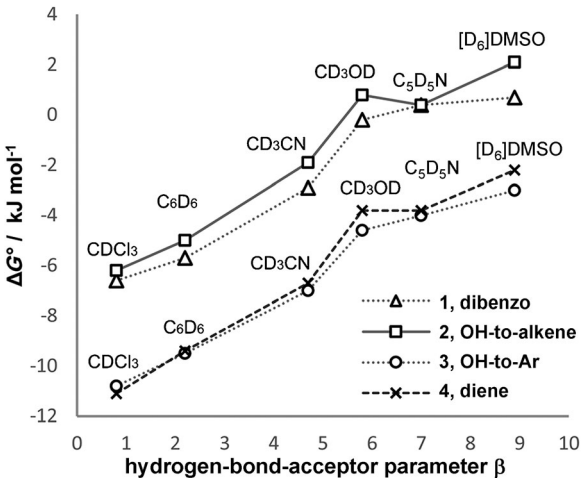

Figure 2. Graph of the free-energy difference $\Delta G° = -RT \ln(p_D/p_U)$ versus the solvent hydrogen bond acceptor parameter β for **1**–**4** with Y = Me, Z = OH. For linear fittings, see Table S7 and Figure S5 in the Supporting Information.

Whilst inspection of the conformational populations can provide interesting insight, the interplay of the counterbalancing functional groups and a more quantitative estimate of the subtle energy difference can be appreciated by visualization in the form of a triple-mutant box,[14] as exemplified for a comparison of the two sets of tertiary alcohols **1**–**4**, Y = Me and Y = CCH, in the solvent methanol (Figure 3). The free-energy differences (ΔΔ*G* values) derived by experiment, together with those from theory (see below) and shown in parenthesis on the 12 edges of the distorted cube, can be grouped into three different subsets.

Thus, the differences in free energy between a π-facial intramolecular hydrogen bond to an arene and to an alkene are shown on the red edges. The measurements for these four different molecular fragments reveal that the OH···π-arene interaction is stronger than the OH···π-alkene interaction by approximately −1.2 kJ mol^{-1} on average for this system. The unfavorable interactions of Y with an alkene relative to an arene are shown in blue, with those for the methyl group (+4.4 and 4.6 kJ mol^{-1}) being considerably higher than for the terminal alkyne (2.4 and 2.6 kJ mol^{-1}), as noted earlier. Finally, as shown in black, the replacement of the methyl group with the terminal alkyne is favored, both for the Y···π arene interaction (−4.1 and −4.7 kJ mol^{-1}) and, even more so, for the Y···π alkene interaction (−6.1 and −6.7 kJ mol^{-1}).

Throughout our studies, the interplay of theory and experiment has always provided additional insight, in particular since a molecular balance is well suited for computational calculation, owing to considerable cancelation of systematic error in the method. According to our recently reported method,[15] which includes dispersion terms and zero-point and entropic corrections on the basis of vibrational partition functions determined by evaluation of solvation corrections with continuous solvent models, the calculated free-energy differences[16] ΔΔ*G*, as defined in Figure 3, are in good agreement with experiment, with a mean error of 1.1 kJ mol^{-1}.

DFT calculations have proven to be of value in understanding the interactions of unsaturated groups with arenes and alkenes. Thus, for the vinyl group (Figure 4), the

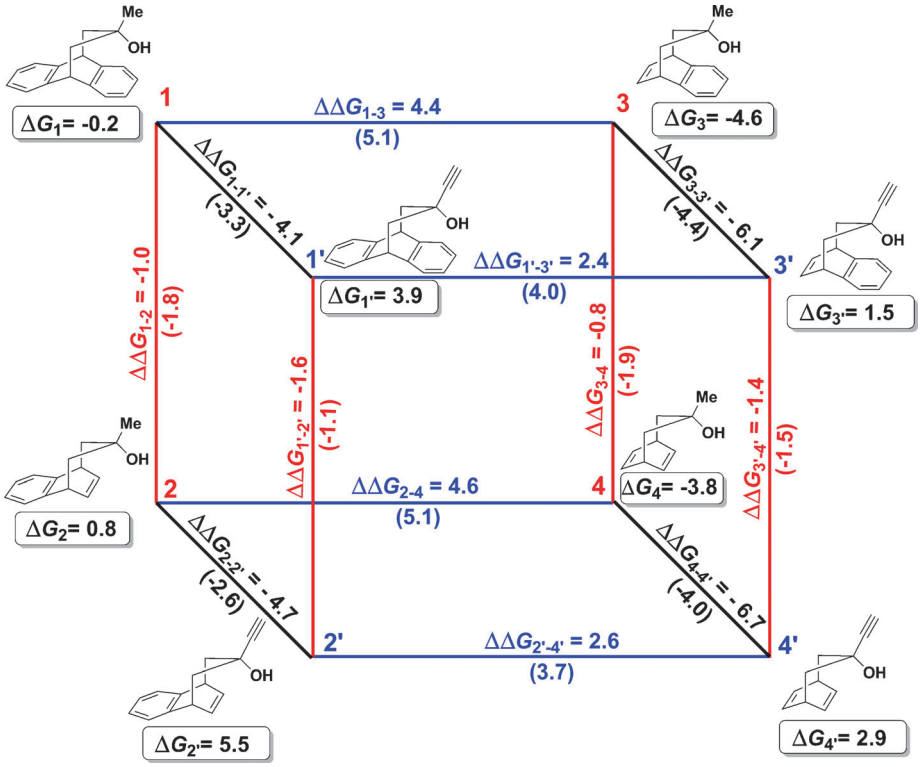

Figure 3. Free energies for **1**–**4** (Y = Me and CCH). Values in parentheses are those computed at the B3LYP + D3/TZVP/SCRF = methanol level.[15,16]

© 2015 Wiley-VCH Verlag GmbH & Co. KGaA, Weinheim

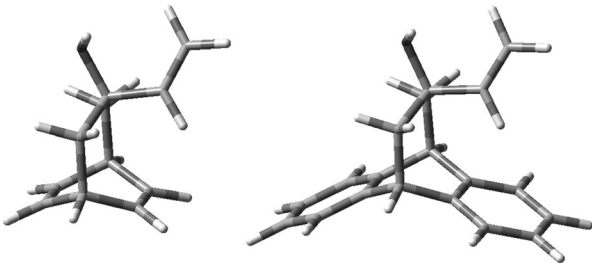

Figure 4. Geometries of **4**U-OH,CH=CH_2 (left) and **1**U-OH,CH=CH_2 (right) from DFT M06-2X/6-31 + G(d) calculations.

preferred conformation is indicative of either an incipient CH···π[17] interaction or an electrostatic interaction with the sp^2-hybridized carbon atom. As expected, face-to-face π stacking is disfavored.

It is, in principle, possible that the C-H···π interaction is stronger for the C(sp^2)–H bond than for the C(sp^3)–H bond. However, a further increase in the p_U value in molecular balances **1**–**4** for Y = C≡CH and C≡N as compared to the CH=CH_2 group (Table 1) is in favor of a simple electrostatic-type interaction between the C^α atom of the Y substituent and the π-acceptor, as the C^α atom becomes more positive on moving from left to right in the sequence of substituents CH_2CH_3, CH=CH_2, C≡CH and C≡N. From our preliminary natural bond orbital (NBO) analysis of M06-2X/6-31 + G(d) calculations of **1**U conformers, the natural charge (q_C, in atomic units) of the C^α atom is −0.49, −0.25, −0.04, and +0.31 in CH_2CH_3, CH=CH_2, C≡CH and C≡N, respectively. The corresponding energetic characteristics, ΔG° values in $CDCl_3$ (see Table S4), show a satisfactory linear dependence on these q_C values (see Figure S4), with $r^2 > 0.9$. This result is in agreement with the known linear dependence of the energy of the electrostatic interaction on the charge ($E \approx q_1 q_2/r$, in which r is the distance between charges q_1 and q_2). These findings support the presence of long-range (r^1-dependent) electrostatic C···π interactions, although further investigations are required to verify the significance of the electrostatic and other interactions.

The noncovalent origin of these free-energy differences can also be visualized by employing the appropriately termed and recently introduced[18] NCI (noncovalent interaction) topological analysis (Figure 5). This analysis presents a view filtered by the value of the electron density to reveal only the properties of the noncovalent regions, and in this region a reduced-density gradient isosurface is color-coded to expose stabilizing regions as blue or green and weakly repulsive regions as yellow (or red). The system Z = OH, Y = CCH nicely illustrates this approach: The interaction between the OH group and the face of a benzo group is rendered as blue, counterbalanced by a weaker (green) surface when the alkyne group interacts with a benzo group, but now a second smaller region is revealed which is not observed when the alkyne group is replaced with a methyl group.

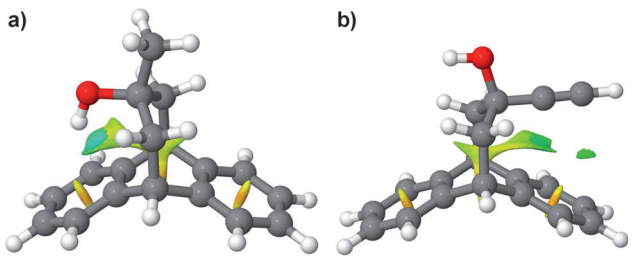

Figure 5. NCI surfaces[18] for Z = OH, Y = CCH illustrating: a) the attractive NCI region between the OH group and the face of the benzo ring, and b) the attractive region between the CCH group and the face of the benzo ring, revealing two distinct attractive areas.

In conclusion, the foregoing results have provided quantitative data to demonstrate that a π-facial intramolecular hydrogen bond from a hydroxy group to an arene is stronger than that to an alkene. The remarkable behavior discovered for the cyano group, which forms an even stronger interaction than the hydroxy group with both an arene and an alkene, is reminiscent of an incipient cation–π interaction and certainly worthy of consideration for π-facial discrimination in drug and catalyst design. Interestingly, comparative analysis of data for Y = CH_2CH_3, CH=CH_2, C≡CH, and C≡N groups is indicative of a weak long-range electrostatic type of C···π interaction with the C^α atom of the Y substituent and the π system.

Received: October 1, 2014
Published online: November 17, 2014

Keywords: conformational analysis · molecular balances · NMR spectroscopy · noncovalent interactions · π interactions

[1] a) L. M. Salonen, M. Ellermann, F. Diederich, *Angew. Chem. Int. Ed.* **2011**, *50*, 4808–4842; *Angew. Chem.* **2011**, *123*, 4908–4944; b) E. A. Meyer, R. K. Castellano, F. Diederich, *Angew. Chem. Int. Ed.* **2003**, *42*, 1210–1250; *Angew. Chem.* **2003**, *115*, 1244–1287; c) R. K. Raju, J. W. G. Bloom, Y. An, S. E. Wheeler, *ChemPhysChem* **2011**, *12*, 3116–3130; d) B. L. Schottel, H. T. Chifotides, K. R. Dunbar, *Chem. Soc. Rev.* **2008**, *37*, 68–83; e) T. Steiner, *Angew. Chem. Int. Ed.* **2002**, *41*, 48–76; *Angew. Chem.* **2002**, *114*, 50–80.

[2] a) C. A. Hunter, J. K. M. Sanders, *J. Am. Chem. Soc.* **1990**, *112*, 5525–5534; b) F. Cozzi, M. Cinquini, R. Annunziata, T. Dwyer, J. S. Siegel, *J. Am. Chem. Soc.* **1992**, *114*, 5729–5733; c) J. H. Williams, *Acc. Chem. Res.* **1993**, *26*, 593–598; d) S. Paliwal, S. Geib, C. S. Wilcox, *J. Am. Chem. Soc.* **1994**, *116*, 4497–4498.

[3] a) S. Burley, G. Petsko, *Science* **1985**, *229*, 23–28; b) M. Hirota, K. Sakaibara, H. Suezawa, T. Yuzuri, E. Ankai, M. Nishio, *J. Phys. Org. Chem.* **2000**, *13*, 620–623.

[4] a) D. A. Dougherty, *Acc. Chem. Res.* **2013**, *46*, 885–893; b) H. Ihm, S. Yun, H. G. Kim, J. K. Kim, K. S. Kim, *Org. Lett.* **2002**, *4*, 2897–2900; c) H. Adams, C. A. Hunter, K. R. Lawson, J. Perkins, S. E. Spey, C. J. Urch, J. M. Sanderson, *Chem. Eur. J.* **2001**, *7*, 4863–4877; d) P. Lakshminarasimhan, R. B. Sunoj, J. Chandrasekhar, V. Ramamurthy, *J. Am. Chem. Soc.* **2000**, *122*, 4815–4816.

[5] a) E.-i. Kim, S. Paliwal, C. S. Wilcox, *J. Am. Chem. Soc.* **1998**, *120*, 11192–11193; b) B. Bhayana, C. S. Wilcox, *Angew. Chem. Int. Ed.* **2007**, *46*, 6833–6836; *Angew. Chem.* **2007**, *119*, 6957–6960.

[6] a) S. L. Cockroft, C. A. Hunter, *Chem. Commun.* **2006**, 3806–3808; b) L. Yang, C. Adam, G. S. Nichol, S. L. Cockroft, *Nat. Chem.* **2013**, *5*, 1006–1010; c) A. Nijamudheen, D. Jose, A. Shine, A. Datta, *J. Phys. Chem. Lett.* **2012**, *3*, 1493–1496; d) P.

© 2015 Wiley-VCH Verlag GmbH & Co. KGaA, Weinheim

Cornago, R. M. Claramunt, L. Bouissane, J. Elguero, *Tetrahedron* **2008**, *64*, 3667 – 3673; e) P. Li, C. Zhao, M. D. Smith, K. D. Shimizu, *J. Org. Chem.* **2013**, *78*, 5303 – 5313; f) C. Zhao, R. M. Parrish, M. D. Smith, P. J. Pellechia, C. D. Sherrill, K. D. Shimizu, *J. Am. Chem. Soc.* **2012**, *134*, 14306 – 14309; g) W. R. Carroll, C. Zhao, M. D. Smith, P. J. Pellechia, K. D. Shimizu, *Org. Lett.* **2011**, *13*, 4320 – 4323; h) W. R. Carroll, P. Pellechia, K. D. Shimizu, *Org. Lett.* **2008**, *10*, 3547.

[7] I. K. Mati, S. L. Cockroft, *Chem. Soc. Rev.* **2010**, *39*, 4195 – 4205.

[8] a) W. B. Motherwell, J. Moïse, A. E. Aliev, M. Nič, S. J. Coles, P. N. Horton, M. B. Hursthouse, G. Chessari, C. A. Hunter, J. G. Vinter, *Angew. Chem. Int. Ed.* **2007**, *46*, 7823 – 7826; *Angew. Chem.* **2007**, *119*, 7969 – 7972; b) A. E. Aliev, J. Moïse, W. B. Motherwell, M. Nič, D. Courtier-Murias, D. A. Tocher, *Phys. Chem. Chem. Phys.* **2009**, *11*, 97 – 100.

[9] G. Desiraju, T. Steiner, *The Weak Hydrogen Bond*: *Applications to Structural Chemistry and Biology*, Oxford University Press, Oxford, **1999**, pp. 185 – 190.

[10] a) B. T. G. Lutz, J. H. van der Maas, *J. Mol. Struct.* **1997**, *436 – 437*, 213 – 231; b) B. Lutz, J. A. Kanters, J. van der Maas, J. Kroon, T. Steiner, *J. Mol. Struct.* **1998**, *440*, 81 – 87; c) A. W. Baker, A. T. Shulgin, *J. Am. Chem. Soc.* **1958**, *80*, 5358 – 5363; d) M. A. Viswamitra, R. Radhakrishnan, J. Bandekar, G. R. Desiraju, *J. Am. Chem. Soc.* **1993**, *115*, 4868 – 4869.

[11] a) H. S. Rzepa, M. H. Smith, M. L. Webb, *J. Chem. Soc. Perkin Trans. 2* **1994**, 703 – 707; b) M. Parvez, *Acta Crystallogr. Sect. C* **1987**, *43*, 1408 – 1410; c) H. E. Zimmerman, M. J. Zuraw, *J. Am. Chem. Soc.* **1989**, *111*, 7974 – 7989.

[12] C. A. Hunter, *Angew. Chem. Int. Ed.* **2004**, *43*, 5310 – 5324; *Angew. Chem.* **2004**, *116*, 5424 – 5439.

[13] a) K. B. Muchowska, C. Adam, I. K. Mati, S. L. Cockroft, *J. Am. Chem. Soc.* **2013**, *135*, 9976 – 9979; b) I. K. Mati, C. Adam, S. L. Cockroft, *Chem. Sci.* **2013**, *4*, 3965 – 3972; c) S. L. Cockroft, C. A. Hunter, *Chem. Commun.* **2009**, 3961 – 3963.

[14] S. L. Cockroft, C. A. Hunter, *Chem. Soc. Rev.* **2007**, *36*, 172 – 188.

[15] A. Armstrong, R. A. Boto, P. Dingwall, J. Contreras-García, M. J. Harvey, N. J. Mason, H. S. Rzepa, *Chem. Sci.* **2014**, *5*, 2057 – 2071.

[16] An interactive data-table with full details of energies and corresponding geometries is available at H. S. Rzepa, A. E. Aliev, J. R. Arendorf, I. Pavlakos, R. B. Moreno, M. J. Porter, W. B. Motherwell figshare. DOI: 10.6084/m6089.figshare.1167503, shortDOI: vmh Retrieved Sep 16, **2014** (GMT).

[17] O. Takahashi, Y. Kohno, M. Nishio, *Chem. Rev.* **2010**, *110*, 6049 – 6076.

[18] a) E. R. Johnson, S. Keinan, P. Mori-Sánchez, J. Contreras-García, A. J. Cohen, W. Yang, *J. Am. Chem. Soc.* **2010**, *132*, 6498 – 6506; b) J. R. Lane, J. Contreras-García, J.-P. Piquemal, B. J. Miller, H. G. Kjaergaard, *J. Chem. Theory Comput.* **2013**, *9*, 3263 – 3266.

 © 2015 Wiley-VCH Verlag GmbH & Co. KGaA, Weinheim